© 2026. Published by The Company of Biologists | Journal of Experimental Biology (2026) 229, jeb251716. doi:10.1242/jeb.251716

RESEARCH ARTICLE

Acute stress modulates early visual perception and decision-making speed in bees

Olga Procenko*,‡ and Vivek Nityananda‡

ABSTRACT

Affective states influence decision making but can also directly affect earlier stages of sensory processing. In humans, exposure to threatening stimuli alters the perception of basic visual features, fine-tuning vision to support faster responses in threatening contexts. Whether similar stressors induce changes in early vision in insects and affect visually guided decision making remains unknown. Here, we examined how stress, induced by a simulated predatory attack known to elicit a negative affective state, affects bumblebee vision and subsequent decision making. We examined the effect of this experience on sensitivity thresholds for two features of spatial vision, resolution and contrast, as well as bumblebee choice dynamics in a dual-choice discrimination task. We found that stress modulated both thresholds: it increased the contrast sensitivity threshold and shifted the spatial frequency threshold toward finer resolution. Stress also modulated subsequent choice behaviour, increasing commitment and accelerating decisions when early perceptual judgments were accurate. Importantly, these faster choices did not compromise accuracy. Collectively, our results suggest that experience of predation reshapes bee visual sensitivity and decision making not only through an increase in reactivity but also via a flexible shift in decision making driven by perceptual confidence.

KEY WORDS: Visual acuity, Vision, Stress, Contrast sensitivity, Spatial frequency, Bumblebees, Emotion, Predation

INTRODUCTION

Visually guided behaviour depends on both external stimuli and an animal's internal state. In insects, a growing body of research shows that vision is modulated by a range of states. For instance, in food-deprived blowflies, walking-induced enhancement of motion interneurons is reduced, possibly to conserve energy when reserves are low (Longden et al., 2014). Similarly, increased insulin levels in praying mantises – often associated with satiety – reduce the range of distances and azimuths at which prey is detected (Bertsch et al., 2019). Arousal in courting *Drosophila* males has been shown to modulate the gain of specific visual projection neurons, increasing their sensitivity to moving objects and enhancing male persistence while courting a female (Hindmarsh Sten et al., 2021). Other studies have observed visual modulation associated with internal states such as locomotion (Maimon et al., 2010; Rosner et al., 2010) and arousal (Maimon et al., 2010). However, the effect of stress and related affective states on insect vision has remained understudied.

In mammals, the effects of stress-induced states on vision have been extensively studied, including in humans and primates. Participants exposed to threatening stimuli not only detect threats more quickly (Bethell et al., 2016; Rued et al., 2019) but also demonstrate enhanced goal-directed visual search performance, even for threat-unrelated objects (Becker, 2009; Kim et al., 2021). Being in a high-vigilance state could therefore enhance the visual system's ability to detect relevant environmental information (Schwarz and Clore, 1983; Zadra and Clore, 2011). Fear can also modulate early visual perception, heighten stimulus-driven attention and, consequently, facilitate visual decision making. For instance, the brief presentation of a fearful face facilitates target detection by enhancing contrast sensitivity (Phelps et al., 2006). Fear also leads to increased sensitivity to low-level spatial frequencies, another crucial component of visual acuity (Bocanegra, 2011; Bocanegra and Zeelenberg, 2009). Similarly, emotional arousal leads to a shift in peak contrast sensitivity towards lower spatial frequencies (Lee et al., 2014). These changes to early vision, therefore, directly influence visual search and suggest an adaptive role in threat detection.

Given the possible adaptive role for these processes, we should expect similar modulation of vision by stress even in insects. Pollinators such as bumblebees rely heavily on vision for navigation and foraging. They are also exposed to multiple stressors, including natural predators and anthropogenic environmental challenges. While stress, and the resultant negative affective state, has been shown to alter bee visual decision making (Procenko et al., 2024), its effects on visual processing remain unexplored. To address this, we investigated whether exposing bees to a task-irrelevant mechanical stressor, thought to simulate predation and known to induce negative affective states in bees (Procenko et al., 2024), influences their visual perception. Specifically, we examined whether this stress modulates the perception of low-level visual features, stimulus contrast and spatial frequency. Bees were trained to discriminate rewarding horizontal sigmoidal gratings from unrewarded vertical ones in a Y-maze set-up. Subsequently, bees were tested on pairs of gratings with varying spatial frequencies and decreasing contrasts to determine their spatial resolution and contrast thresholds. We hypothesised that exposing bees to acute stress, and the resultant negative states, would lead to a shift in contrast and spatial resolution thresholds.

MATERIALS AND METHODS

Animals and housing

We used four commercially raised *Bombus terrestris* (Linnaeus 1758) colonies (Agralan, The Old Brickyard, Wiltshire, UK) that were transferred to bipartite plastic nest-boxes (28.0×16.0×12.0 cm). The nest-box was connected to the custom-built Y-maze via a transparent

Biosciences Institute, Newcastle University, Henry Wellcome Building, Framlington Place, Newcastle upon Tyne NE2 4HH, UK.
*Present address: School of Biosciences, University of Birmingham, Birmingham B15 2TT, UK

‡Authors for correspondence (p.olga@bham.ac.uk; vivek.nityananda@newcastle.ac.uk)

O.P., 0000-0002-3929-4320; V.N., 0000-0002-2878-2425

Received 7 October 2025; Accepted 3 May 2026

acrylic tunnel (56.0×5.0×5.0 cm), with shutters controlling bee access to the maze. Bees were kept at 23±2°C, with double LED tubes (Philips CorePro, 600 mm, 8 W T8) providing uniform illumination in the Y-maze: 1100 lx in both arms and 1020 lx at the entrance (measured by digital light meter, LX1010BS, Dr.meter).

Throughout the experimental period, colonies were fed with ∼3 g commercial pollen daily (Koppert B.V., Berkel en Rodenrijs, The Netherlands) and provided with sucrose solution (20% w/w) *ad libitum* with a gravity feeder on non-experimental days. Bees were food deprived prior to training or testing. Although invertebrates do not fall under the UK Animals (Scientific Procedures) Act, 1986 (ASPA), the experimental design and protocols were developed incorporating the 3Rs principles. Housing, maintenance and experimental procedures were non-invasive and were kept as close as possible to the natural living conditions of the animals. This project was approved by Newcastle University's ethics board (reference number: 8666/2020).

Training apparatus

The Y-maze design followed the specifications of a previously published experiment designed for measuring visual acuity in *B. terrestris* (Chakravarthi et al., 2016). The Y-maze comprised three identical arms, each measuring 20 cm in height, width and length, and covered with UV-transparent Plexiglas sheets (see Fig. 1A). Two of these three arms served as decision arms, while the third functioned as the entrance arm. The entrance arm contained a transparent Plexiglas tunnel (3 cm×3 cm×3 cm), which connected to the other two arms within the maze. This tunnel in the entrance arm provided direct access to an outer tunnel leading to the nest-box. The rear wall of each decision arm was equipped with a hole (1 cm in diameter) used for the insertion of a reward chamber.

Stimuli

Stimuli were identical to those used in a previous study (Chakravarthi et al., 2016), and consisted of achromatic sinusoidal gratings with pattern wavelengths of 6.6, 5, 2.5, 1.53, 1.25, 1.0 and 0.5 cm, corresponding to spatial frequencies of 0.035, 0.070, 0.140, 0.280, 0.437 and 0.699 cycles deg^{-1} of visual angle at the 20 cm decision line (see Fig. 1A). Patterns with spatial frequency of 0.070 cycles deg^{-1} and 87% contrast were used for training because they have previously been shown to be the easiest for bees to resolve (Chakravarthi et al., 2016). For the contrast sensitivity experiments, we used gratings with a fixed spatial frequency of 0.070 cycles deg^{-1}, with varying Michelson contrasts of 87%, 68%, 54%, 39% and 22%. For the spatial resolution experiment, we used gratings of varying spatial frequencies of 0.035, 0.070, 0.140, 0.280, 0.437 and 0.699 cycles deg^{-1} at a fixed Michelsen contrast of 87%.

Training and testing procedure

Pre-training

Bees foraging on the feeder were marked with a paint marker (Edding 750) and later recruited for training. To familiarise individual bees with the two reward chambers, each bee was captured at the maze entrance using a cup and guided into a chamber by aligning it with the entrance, forcing the bee to enter and discover a 0.2 ml droplet of 50% (w/w) sugar solution. This procedure was repeated twice for each reward chamber for a total of four trials. During pre-training, bees were presented with the training grating pair (spatial frequency of 0.070 cycles deg^{-1} and 87% contrast) for the first time: one positioned horizontally and the other vertically, with one grating in each arm (see Fig. 1A). Throughout the experiment, the horizontal grating was always associated with a reward, and the vertical grating with water. During pre-training, the initial presentation of the rewarding horizontal grating was randomised across bees. Subsequently, the side of this grating in the three following pre-training trials was alternated based on the initial presentation sequence (e.g. L–R–L–R or R–L–R–L).

Training

After the forced-choice pre-training phase, we began the training phase where bees were allowed to access the reward chamber freely. As before, on each training trial, bees were presented with horizontal and vertical grating positioned in the decision arms. The reward chamber on the arm with the horizontal grating contained a sugar reward (0.2 ml, 50% w/w), while the reward chamber on the side of the vertical grating contained distilled water (0.2 ml). The side of the rewarding horizontal grating was pseudorandomised across trials, with no more than two consecutive presentations of the horizontal grating on the same side. A new pseudorandom sequence was generated for each bee in R by using the *sample()* function. During training and testing, reward chambers were changed each trial to provide fresh sucrose/distilled water and remove scent marks. Chambers were washed with 70% ethanol and hot water, then dried before the next experimental day.

In previous visual acuity experiments (Chakravarthi et al., 2016), a stationary point at the entrance to the maze was used as the decision point. However, we observed that some bees walked down instead of taking off immediately upon entering the tunnel. Therefore, this entrance stationary point was considered ineffective as a decision point for the study. To avoid inaccurate measurements and following other studies (e.g. Spaethe and Chittka, 2003), the choice point was defined as the first crossing of the 20 cm decision line in either of the two decision arms. This adjustment allowed bees to navigate a small triangular area after entering but before making their choice. Bees that successfully learned to distinguish between the horizontal and vertical grating and met the learning criterion (80% accuracy in the last 20 trials) proceeded to the testing phase.

Testing

Each bee underwent a total of 13 test trials. Each test trial consisted of the presentation of one vertical and one horizontal grating with identical spatial frequencies and contrast levels. To assess tuning to spatial frequencies, each bee was tested on six distinct spatial frequencies in separate test trials, all at a fixed maximum contrast of 87%. The six spatial frequencies used were 0.035, 0.070, 0.140, 0.280, 0.437 and 0.699 cycles deg^{-1}. Of these spatial frequencies, three (0.280, 0.437 and 0.699 cycles deg^{-1}) were tested twice for each bee, as they are less effectively resolved by bumblebees (Chakravarthi et al., 2016). To assess contrast sensitivity, bees were presented with gratings featuring a fixed spatial frequency of 0.070 cycles deg^{-1} but with varying contrasts of 87%, 68%, 54%, 39% and 22%, in separate trials. As before, the bee's choice was recorded when it crossed the decision line for the first time. Additionally, the final decision of the bee, i.e. entering a reward chamber, was also recorded. Bees failing to enter either reward chamber within a 120 s period were categorised as 'omissions' from making a final choice.

All test trials were unrewarded, with both reward chambers containing 0.2 ml of distilled water. As with training, for each bee, test stimuli were also presented in a randomised order generated *a priori* in R. To keep bees motivated, a set of refresher trials was performed after each test. Each refresher block consisted of two presentations of the grating pair used for training, with a rewarding horizontal grating placed once in each arm in each of the presentations. Bees that failed to enter the reward chamber in the

Journal of Experimental Biology (2026) 229, jeb251716. doi:10.1242/jeb.251716

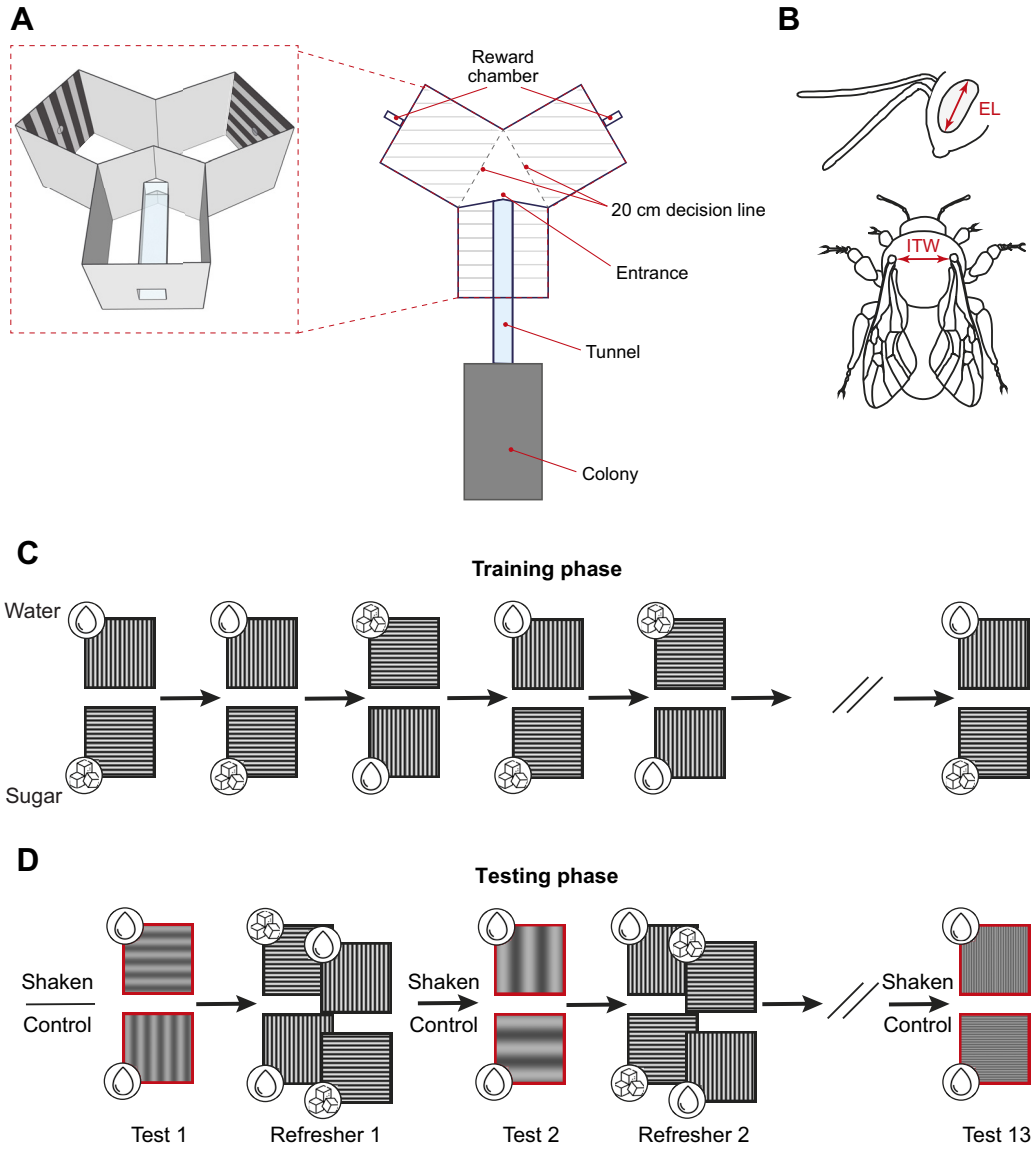

Fig. 1. Experimental setup and morphological measurements. (A) Experimental setup and stimuli. Bees accessed the decision arms through the entrance at the end of the tunnel. Both decision arms (20×20×20 cm) contained openings that led to a rewarding chamber which bees had to enter in order to sample its contents. During training and testing trials, achromatic sinusoidal gratings (horizontal or vertical) were positioned on the back wall of each decision arm. The choice was determined by the first crossing of the 20 cm decision line in either of the two decision arms. (B) Morphological measurements included the length of the compound eye (EL) and the intertegular width (ITW). (C) Training protocol. Bees chose between the rewarding horizontal (sugar solution) and non-rewarding vertical grating (water), with the rewarded side pseudorandomised for each bee. Bees achieving the learning criterion (≥80% correct in the final 20 trials) proceeded to testing. (D) Testing protocol. Bees were presented with unrewarded grating pairs varying in contrast and spatial frequency. Each bee was tested with 13 stimulus pairs in randomised order, with each test trial followed by two refresher trials using the training stimulus, in which the rewarded horizontal grating was presented once on each side in random order. Before each test trial, bees were either shaken or left unmanipulated (control).

correct arm, indicated by the horizontal grating, after a maximum of three refresher blocks were eliminated from the test trial. In total, 3 bees (1 control, 2 shaken) were excluded.

Predatory attack simulation

Prior to testing, individual bees were randomly allocated to one of two groups: a shaking treatment thought to simulate predator-related disturbance (n=20) or an unmanipulated group that served as a control (n=20). The bees in the shaken group were individually subjected to 60 s of shaking at 1200 rpm using a Vortex-T Genie 2 (Procenko et al., 2024). This treatment has been suggested to resemble the shaking of a colony by a bear or honey badger (Bateson et al., 2011; Schlüns et al., 2017). Before entering the flight arena, we allowed the bee to enter a custom-made tagging cage softened by sponge to prevent physically harming them while shaking (40 mm diameter, 7.5 cm length). After entering, the bee was gently nudged down with a soft foam plunger until the distance between the plunger and the bottom of the cage was reduced to ∼3 cm. Once the plunger was secured, the cage with the bee was placed inside the vortex cup head. We then ran the Vortex at 1200 rpm for 60 s to shake the bee. After the shaking treatment, we released the bee into the tunnel connected to the Y-maze via an opening on the top of the tunnel. The bee was allowed to enter the Y-maze for testing as soon as it was ready to initiate a foraging bout (up to a maximum

time of 60 s). Bees in the shaken group experienced the shaking procedure before each test trial. After completing all tests, the bee was frozen and stored in 70% ethanol at −20°C. Morphometric measurements, including the length of the compound eye and the intertegular width (see Fig. 1B), were next taken, as earlier studies suggested object resolution is dependent on body size (Spaethe and Chittka, 2003). The measurements were taken under a dissecting microscope using a digital calliper (RS PRO Digital Calliper, 0.01±0.03 mm).

Video analysis

All test trials were recorded using a Huawei Nexus 6P phone with a 1440×2560 pixel resolution, capturing video at 120 frames s^{-1}. Subsequently, we used the video analysis program BORIS 7.10.2107 (Friard and Gamba, 2016) to analyse the recorded videos and extract information about bee choices. Specifically, the following time points were coded during analysis: (1) the bee entering the Y-maze, (2) the bee crossing the decision line and (3) the bee entering the reward chamber. These coded time points were used to determine which arm was entered when the decision line was crossed, and which reward chamber was entered. They were also used to calculate latencies for both decisions.

Statistical analysis

The hypothesis and statistical analyses of the main experiment were preregistered at the platform AsPredicted (https://aspredicted.org/48w4-b3kw.pdf). The data were plotted and analysed using RStudio v.3.2.2 (The R Foundation for Statistical Computing, Vienna, Austria, http://www.r-project.org) and custom-written scripts. To determine the thresholds for contrast sensitivity and spatial resolution, we fitted a logistic psychometric function (*quickpsy*, 'quickpsy' package; Linares and López-Moliner, 2016) to the binomial choice data of the bees. In this model, a choice of 1 indicates crossing the decision line in the arm with the rewarding stimulus (hereafter rewarding arm), while a choice of 0 indicates crossing in the arms with the unrewarding stimulus (hereafter non-rewarding arm). The psychometric function is defined as:

$$\psi(x) = \gamma + (1 - \gamma - \lambda)\left(1 + e^{\left(\frac{a-x}{b}\right)}\right)^{-1}, \quad (1)$$

where $\psi(x)$ represents the proportion of correct choices across different spatial frequencies or contrasts; the parameter γ represents chance performance and was held constant at 0.5, while the parameter λ accounts for stimulus-independent error or lapse rate, allowing for variability (set as 'TRUE') (Linares and López-Moliner, 2016). The function was fitted using a maximum likelihood method and parametric bootstrapping to estimate confidence intervals.

We fitted a generalised mixed effect model (GLMM) with a binomial error distribution and a logit link function (*glmmTMB*, 'glmmTBM' package; Magnusson et al., 2017) to assess whether shaking modulated a bee's ability to discriminate between horizontal and vertical patterns with decreasing contrasts and varying spatial frequencies. While the effects of spatial frequency and contrast were analysed separately, the response variable in all sets of models was choice accuracy (coded as 1 for crossing the decision line in the correct arm with horizontal grating and 0 for crossing the decision line in the incorrect arm with vertical grating). For the analysis of the effects of contrast, the explanatory variables were Michelson contrast ('Contrast', coded as a continuous variable and including all five contrasts: 22%, 39%, 54%, 68% and 87%), treatment ('Treatment', coded as a factor with two levels: control and shaking) and bee eye width ('Eye width', coded as a continuous variable). For the analysis of the effect of spatial frequency, the explanatory variables were spatial frequency ('Frequency', coded as a factor of six levels: 0.699, 0.437, 0.280, 0.140, 0.070 and 0.035 cycles deg^{-1}), treatment ('Treatment', coded as a factor with two levels: control and shaking) and bee eye width ('Eye width', coded as a continuous variable). In all models, the identity of the bee ('ID') was included as a random intercept variable.

Both initial choice (crossing the decision line) and final choice (entering the reward chamber) latency were modelled using a linear mixed effect model (LMEM) (*lmer*, 'lme4' package; Bates et al., 2015). As before, the effects of spatial frequency and contrast were analysed separately. Prior to analysis, we performed log or reciprocal transformations for the initial and final choice latencies, respectively, as the latency data were right skewed. To assess whether shaking affected the latency (either initial or final) on the trials with decreasing contrast, the explanatory variables were Michelson contrast ('Contrast', coded as a factor of five levels: 22%, 39%, 54%, 68% and 87%) and treatment ('Treatment', coded as a factor with two levels: control and shaking). To analyse the effect of varying spatial frequencies, the explanatory variables were spatial frequency ('Frequency', coded as a factor of six levels: 0.699, 0.437, 0.280, 0.140, 0.070 and 0.035 cycles deg^{-1}), treatment ('Treatment', coded as a factor with two levels: control and shaking) and bee eye width ('Eye width', coded as a continuous variable). As before, in all models, the identity of the bee ('ID') was included as a random intercept variable.

The final choice of reward chamber in each test was categorised according to three mutually exclusive choice categories: choosing a reward chamber on the side with horizontal grating (correct), choosing a reward chamber on the side with vertical grating (incorrect), and omission of response (omission). Response omission was recorded if the bee did not enter either reward chamber for longer than the cut-off criterion of 120 s. Each choice was transformed into a binary response variable for each choice category. Thus, if a bee entered a reward chamber in the correct arm with horizontal grating, the choice was recorded as (1, 0, 0) for a choice of the correct, incorrect and omission, respectively. Choices were analysed using GLMM using the *glmer* function of the 'lme4' package with binomial errors and a logit link function (Bates et al., 2015). The independent variables (fixed factors) were the treatment group ('Treatment') and the choice category ('Choice'). As before, the identity of the bee ('ID') was included as a random factor.

For each response variable, the model selection process comprised comparing models with and without all possible interactions between explanatory variables. The most appropriate model was selected based on the Akaike information criterion (AIC) scores. We considered the model with the lowest AIC score the best model, i.e. the model that provides a satisfactory explanation of the variation in the data (Johnson and Omland, 2004). Models with an AIC difference of less than 2 were considered not significantly better than the model it was being compared with (Burnham and Anderson, 2002). In such cases, the *anova()* function was used to determine whether adding interaction terms significantly improved model fit. We used the 'DHARMa' package (https://CRAN.R-project.org/package=DHARMa) for model diagnostics. For each final model, the significance of fixed effects and interactions was assessed using analysis of variance with Wald chi-square tests using the *Anova* function of the 'car' package (Fox et al., 2019). Additional model summaries were inspected to extract coefficient estimates, standard errors and associated *z*- or *t*-values for fixed effects. If a significant interaction was detected, *post hoc* comparisons were conducted using the 'emmeans' package (https://CRAN.R-project.org/package=emmeans) with Bonferroni adjustment for multiple comparisons.

Journal of Experimental Biology (2026) 229, jeb251716. doi:10.1242/jeb.251716

RESULTS

Morphometric measurements of shaken and control bees

The intertegular width of the bees ranged from 3.62 to 4.27 mm for control bees [median±interquartile range (IQR): 3.88±0.352 mm] and from 3.65 to 4.19 mm for shaken bees (median±IQR: 4.02±0.238 mm). The eye length fluctuated between 2.52 and 2.79 mm for control bees (median±IQR: 2.64±0.142 mm) and 2.42 and 2.90 mm for shaken bees (median±IQR: 2.71±0.137 mm). In line with previous studies (Spaethe and Chittka, 2003), the correlation between these two measures was statistically significant (control: r=0.75, P=0.0002; shaken: r=0.70, P=0.0005). While intertegular width did not differ significantly between groups (W=160, P=0.399), eye length showed a moderate difference (W=118, P=0.044, r=0.32). Given the strong correlation between the two morphological traits and the significant difference in eye length, the latter was used to control for size-related variation that could explain the observed effects. Consequently, eye length was included as an explanatory factor in subsequent models assessing bee performance.

Shaken bees have higher contrast thresholds and a shift of spatial resolution threshold towards higher frequencies

Contrast threshold

The contrast threshold was determined by fitting a logistic function to the proportion of correct choices made at the decision line. The data included trials where gratings were expressed at five contrasts (87%, 68%, 54%, 39% and 22%) with a fixed spatial frequency of 0.070 cycles deg^{-1}. A value of 80% correct choices was chosen to measure the threshold for both the control and shaken treatment groups, as this value was exceeded at most contrasts (see Fig. 2A). The control group had a contrast threshold of 22.10% Michelson contrast, while the shaken group had lower contrast sensitivity, with a higher contrast threshold of 35.93%. These results suggest that shaken bees have worse discriminability at lower contrasts, as they require a higher contrast threshold to achieve the same level of performance as the control bees.

Spatial resolution threshold

To determine the spatial resolution threshold, we fitted a logistic function to the proportion of correct choices made at a decision line. Here, data included trials with gratings of varying spatial frequencies (0.035, 0.070, 0.140, 0.280, 0.437 and 0.699 cycles deg^{-1}), and fixed contrast (87%). Because of the relatively poor performance, especially at higher spatial frequencies (see Fig. 2C), a value of 65% correct choices was set to measure the threshold for both the control and shaken treatment groups. Although lower than the one used for contrast sensitivity, this value remained significantly above chance (binomial test, χ^2=8.41, d.f.=1, P=0.0037).

For control bees, the spatial resolution threshold for discriminating between vertically and horizontally oriented sinusoidal grating patterns was determined to correspond to a spatial frequency of 0.236 cycles deg^{-1}. However, the spatial resolution for shaken bees was higher, with a spatial frequency of 0.344 cycles deg^{-1}. Therefore, while control bees were able to distinguish gratings expressed in three out of six tested spatial frequencies (0.035, 0.07, 0.140 cycles deg^{-1}) with an accuracy above 65%, shaken bees demonstrated the capacity to discriminate patterns expressed at even higher spatial frequencies,

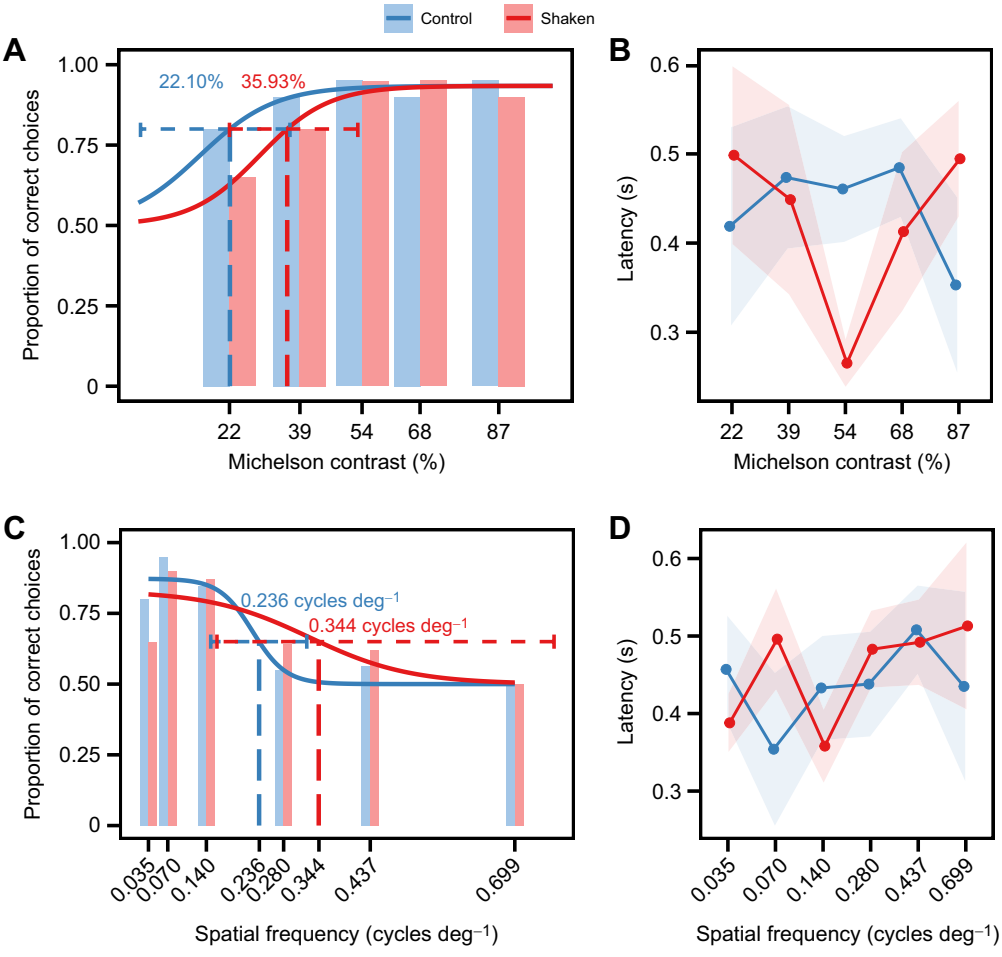

Fig. 2. Shaken bees have higher contrast thresholds and a shift of spatial resolution threshold towards higher frequencies. (A,C) Proportion of correct choices made by control (blue, n=20) and shaken (red, n=20) bees at the decision line for contrast sensitivity (A) and spatial resolution (C) tests. Dashed lines indicate the performance thresholds derived from the fitted logistic functions (blue solid line, control; red solid line, shaken). Error bars show the 95% confidence interval for the threshold. (B,D) Average latency to cross the decision line for control (blue, n=20) and shaken (red, n=20) bees in the contrast sensitivity (B) and spatial resolution (D) tests. Latencies are presented as median values with shaded areas indicating the 95% confidence interval.

including all three that control bees could discriminate (0.035, 0.07, 0.140 cycles deg^{-1}), as well as 0.280 cycles deg^{-1}. A spatial resolution of 2.91 deg in shaken bees suggests they can distinguish finer details and patterns at a smaller angular size than the control group, whose spatial resolution was 4.26 deg.

Shaking does not affect initial choice accuracy or choice latency at the decision line

Effect of contrast sensitivity

Surprisingly, bees demonstrated remarkable accuracy in distinguishing between horizontal and vertical gratings, even when tested at lower contrast levels (see Fig. 2A). Despite the high performance, the contrast threshold for shaken bees was found to be higher (Fig. 2A). We therefore wanted to determine whether this higher contrast threshold had a substantial impact on their overall accuracy in crossing the 20 cm decision line.

The best-fitting model included treatment, contrast and eye length as fixed predictors without any interaction terms (see Table S1). As contrast levels increased, there was a corresponding increase in the likelihood of bees making the correct choice (model estimate ±s.e.=0.030±0.011, z=2.761, P<0.01). Importantly, this trend was consistent across both treatment groups, as shaken bees showed no significant difference in their likelihood of making the correct choice compared with control bees (model estimate±s.e.=−0.410 ±0.505, z=−0.811, P=0.417). Eye length also was not a significant predictor of the response accuracy (model estimate±s.e.=−0.498 ±2.309, z=−0.216, P=0.8291). This finding demonstrates the ability of bees to maintain discrimination accuracy even as contrast levels decreased, irrespective of their treatment group.

We also explored whether there was variation in the time it took for bees to cross the decision line. The best-fitting model for the choice latency analysis included treatment and contrast as fixed factors and an interaction term (see Table S2). Fixed effects of contrast (χ^2=8.84, d.f.=4, P=0.065) and treatment (χ^2=0.025, d.f.=1, P=0.874) were not significant. However, the effect of treatment was contrast dependent (χ^2=12.69, d.f.=4, P=0.013), with shaken bees making significantly faster choices only at a contrast of 54% (t=2.697, P=0.008) (Fig. 2B).

Effect of spatial frequency

When examining the accuracy of bee performance in crossing the decision line in trials with varying spatial frequency, the best-fitting model included treatment, spatial frequency and eye width as fixed predictors without any interaction between factors (see Table S3). Unlike the linear relationship observed with contrast levels (as contrast decreased, accuracy also decreased), the response to varying frequency displayed a different pattern. The highest accuracy was expected at 0.07 cycles deg^{-1} (conditioned resolution), with a decline in accuracy for both higher and lower frequencies. This was precisely the pattern we observed (Fig. 2C). When keeping a spatial frequency of 0.07 cycles deg^{-1} as a reference group, the performance of bees decreased at the lowest (frequency 0.035 cycles deg^{-1}, model estimate±s.e.=−1.480±0.717, z=−2.064, P=0.039) as well as the three highest spatial frequencies (frequency 0.28 cycles deg^{-1}, model estimate±s.e.=−2.200±0.658, z=−3.342, P<0.001; frequency 0.437 cycles deg^{-1}, model estimate±s.e.=−2.210±0.660, z=−3.347, P<0.001; frequency 0.699 cycles deg^{-1}, model estimate±s.e.= −2.682±0.700, z=−3.383, P<0.001). At the same time, bees showed no decrease in accuracy when presented with gratings at a spatial frequency of 0.14 cycles deg^{-1}, which is double their trained frequency of 0.07 cycles deg^{-1} (model estimate±s.e.=−0.723±0.693, z=−1.043, P=0.297). This suggests that this lower frequency is well within the bees' resolvable range and does not impair discrimination. Once again, shaking did not affect the likelihood of crossing the correct decision line (model estimate±s.e.=0.298±0.328, z=0.906, P=0.3650). Similarly, eye width did not significantly affect bee accuracy either (model estimate±s.e.=−2.890±1.579, z=−1.830, P=0.0672).

We further examined whether the decreased accuracy observed at lower and higher spatial frequencies also led to an increase in latency of crossing the decision line and whether shaking impacted this latency. The best-fitting model for assessing the latency to cross the decision line included treatment and spatial frequency as fixed predictors without considering their interaction (see Table S4). Shaking had no statistically significant effect on crossing latency during trials with varying spatial frequency (model estimate±s.e.= 0.037±0.119, t=0.309, P=0.759). Bees took longer to make their choice and cross the decision line at higher spatial frequencies when compared with the trained spatial frequency of 0.07 cycles deg^{-1} (Fig. 2D), which is easily resolvable. Choice latency was significantly higher when the grating had a spatial frequency of 0.699 cycles deg^{-1} (model estimate±s.e.=0.229±0.107, t=2.138, P=0.033). Notably, these were also the spatial frequencies at which bees were less likely to cross the decision line in the correct arm (Fig. 2C). Therefore, the increase in choice latency on these trials may indicate a lack of certainty at these highest spatial frequencies.

Effect of shaking on final choices

Using a two-arm Y-maze allows assessment not only of animals' early perceptual choices (i.e. initial crossing of the decision line) but also of their subsequent decision making, as indicated by entry into the reward chamber. As the arms were not physically separated, bees could freely adjust their flight path and switch to the alternative one if needed. Given the opportunity to gather more information by getting closer to the grating, early perceptual decisions could either be confirmed or corrected. Longer choice latencies have also been linked to lower confidence levels (Kiani et al., 2014). We therefore measured the time taken to enter the reward chamber, i.e. the final choice latency. To account for cases where bees did not choose even after inspection of both gratings at a close distance, we set a time limit of 120 s. Bees that took longer than this cut-off time were considered to be omitting a choice. This approach resulted in three possible decision outcomes: correct choice, incorrect choice or choice omission. First, we assessed whether stress affects bees' willingness to make a choice, and thus their likelihood of falling into one of three outcome categories. We then examined whether perceptual accuracy at the initial decision line modulated decision-making speed for the final choice on trials where a choice was made.

Fixed spatial frequency and varying contrast

The final model for the likelihood of choices included choice category and treatment as factors (see Table S5). Overall, bees were less likely to make incorrect choices (model estimate±s.e.= −3.255±0.269, z=−12.084, P<0.0001) or omit a choice (model estimate±s.e.=−6.149±0.736, z=−8.363, P<0.0001) compared with making correct choices. The likelihood of making any choice (correct, incorrect or omission) was also unaffected by shaking (model estimate±s.e.=−0.021±0.265, z=−0.078, P=0.938) (Fig. 3B).

The best-fitting model for assessing final choice latency (entering a reward chamber) included contrast, treatment and accuracy as fixed factors only (see Table S6). As anticipated, with decreasing contrast levels, bees took longer to enter one of the two reward chambers (model estimate±s.e.=0.003±0.001, t=4.830, P<0.001) (Fig. 3A). Interestingly, early perceptual choice accuracy (i.e.

Journal of Experimental Biology (2026) 229, jeb251716. doi:10.1242/jeb.251716

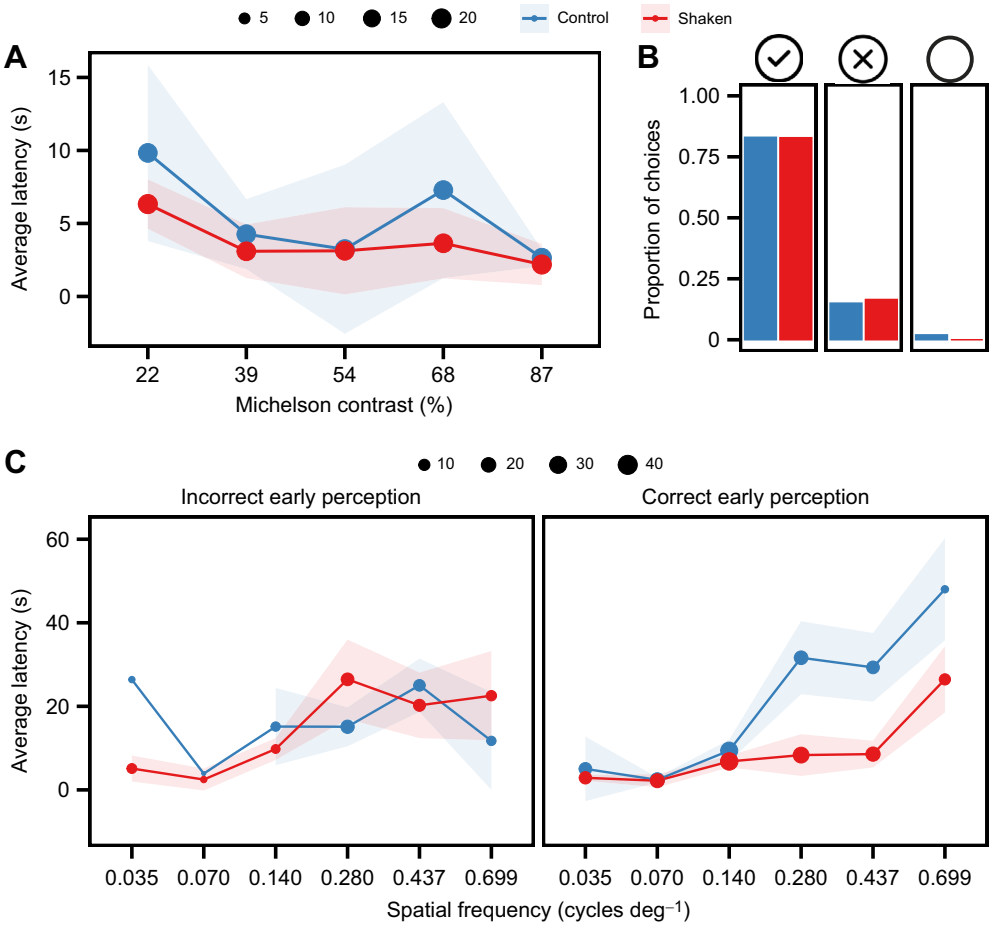

Fig. 3. Stress affects speed of final decisions across spatial frequency but not contrast. (A) Latency to make correct choices across contrasts for control (blue, *n*=20) and shaken (red, *n*=20) bees. Dots represent median values with shaded areas indicating 95% confidence intervals; dot size reflects the number of bees contributing to each median. (B) Proportion of correct choices (left, tick), incorrect choices (middle, cross) and omissions (right, open circle) for control (blue, *n*=20) and shaken (red, *n*=20) bees in varying-contrast trials. (C) Latency to enter the reward chamber after incorrect (left) or correct (right) early perception decisions (i.e. crossing the decision line) across spatial frequencies for control (blue, *n*=20) and shaken (red, *n*=20) bees. Dots represent median values with shaded areas indicating 95% confidence intervals; dot size reflects sample size.

crossing the initial decision line in the correct arm) had no significant effect on how long bees took to make their final choice (model estimate±s.e.=0.036±0.041, t=0.886, P=0.377). Additionally, shaking had a marginally non-significant effect on the final choice latency, despite trending towards a faster decision (model estimate ±s.e.=0.069±0.038, t=1.807, P=0.079). Taken together, these results suggest that as stimulus ambiguity decreases with increasing contrast, decision confidence increases. This increase, however, does not further facilitate decision making. Interestingly, although not statistically significant, stress may contribute to an overall increase in decision speed, but had no effect on the likelihood of specific decision outcomes (correct, incorrect or omission).

Fixed contrast and varying spatial frequency

When assessing the likelihood of decision outcome (correct, incorrect or omissions), the best-fitting model included choice category, treatment and an interaction between these factors (see Table S7). Unlike with the varying contrast trials, the likelihood of a particular choice depended on whether the bee had been shaken or not (χ^2=9.775, d.f.=2, P=0.008). Shaken bees were overall more likely to enter the correct reward chamber compared with control bees (model estimate±s.e.=−0.518±0.261, z=−1.986, P=0.047) and less likely to omit a response (model estimate±s.e.=1.218±0.524, z=2.323, P=0.020) (Fig. 4A).

The best-fitting model for the latency data included spatial frequency, treatment and accuracy at the decision line as fixed factors, with a significant interaction between treatment and accuracy (see Table S8). When keeping the spatial frequency of 0.07 cycles deg^{-1} (learner resolution) as a reference group, the latency to enter the reward chamber significantly increased for all other spatial frequencies (frequency 0.035 cycles deg^{-1}, model estimate±s.e.= 0.782±0.197, t=3.964, P<0.0001; frequency 0.140 cycles deg^{-1}, model estimate±s.e.=1.154±0.170, t=6.798, P<0.0001; frequency 0.280 cycles deg^{-1}, model estimate±s.e.=1.770±0.174, t=10.165, P<0.0001; frequency 0.437 cycles deg^{-1}, model estimate±s.e.=1.915 ±0.179, t=10.719, P<0.0001; frequency 0.699 cycles deg^{-1}, model estimate±s.e.=2.163±0.212, t=10.218, P<0.0001). The effect of treatment, while not significant alone, was dependent on early perceptual decisions (χ^2=7.14, d.f.=1, P=0.008), with shaken bees making significantly faster final choices after crossing the correct decision line (t=4.176, P=0.0001) but not the incorrect one (t=0.044, P=0.965) (Fig. 3C).

Faster decisions are not always accurate (Chittka et al., 2003). We, therefore, next asked whether final choice latencies could predict choice accuracy and, if so, whether or not this was facilitated by stress. The best-fitting model for final choice accuracy data included spatial frequency, choice latency and treatment as fixed factors, as well as an interaction between choice latency and spatial frequency (see Table S9). While choice latency was a significant predictor (χ^2=5.77, d.f.=1, P=0.016) of final choice accuracy, the significant interaction with spatial frequency indicated that its effect varied across spatial frequency conditions (Fig. 4B; χ^2=11.14, d.f.=5, P=0.049). Specifically, longer choice durations were significantly associated with decreased accuracy at mid-range spatial frequencies (0.14 cycles deg^{-1}: slope estimate±s.e.=−0.081±0.029, P=0.0057; 0.28 cycles deg^{-1}: slope estimate±s.e.=−0.037±0.017, P=0.032). While not statistically significant, a negative slope was estimated for several other frequencies as well. However, at the finest spatial

Journal of Experimental Biology (2026) 229, jeb251716. doi:10.1242/jeb.251716

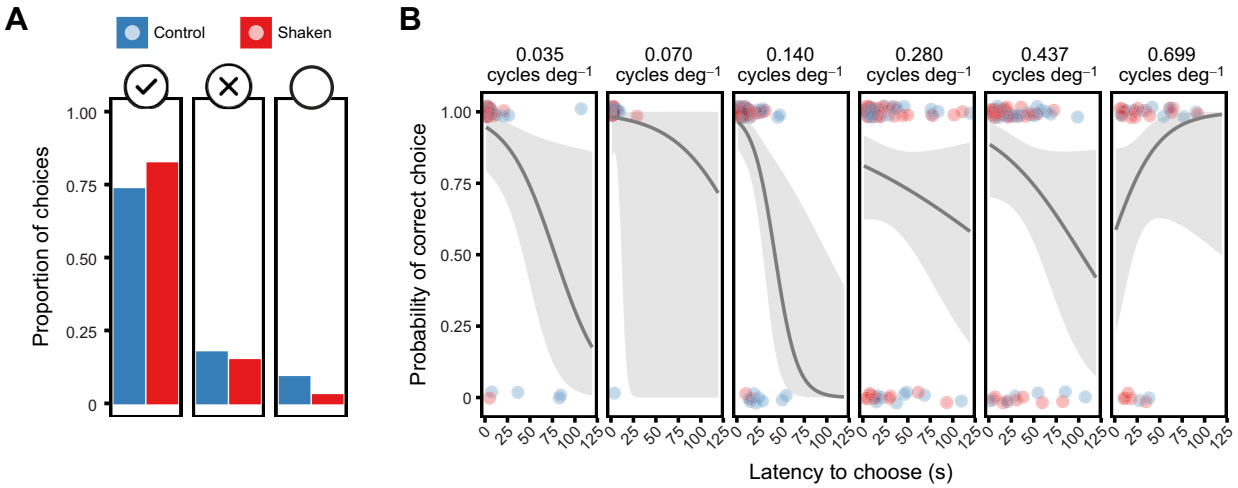

Fig. 4. Latency and stress modulate final choice accuracy across spatial frequencies. (A) Proportion of correct final choices (left, tick), incorrect choices (middle, cross) and omissions (right, open circle) for control (blue, *n*=20) and shaken (red, *n*=20) bees in trials with varying spatial frequencies. (B) Model-predicted relationship between final choice latency and accuracy at each spatial frequency. Coloured points represent observed trial outcomes (1=correct, 0=incorrect) for each control (blue, *n*=20) and shaken (red, *n*=20) bee. The grey line depicts the predicted probability of a correct choice from the binomial GLMM, with shaded 95% confidence intervals. The training stimulus had a spatial frequency of 0.070 cycles deg^{-1}.

frequency (0.699 cycles deg^{-1}), the trend reversed, showing a non-significant positive association, suggesting that in this condition, longer choice latencies may be associated with increased accuracy (slope estimate±s.e.=0.037±0.025, P=0.137) (Fig. 4B). Interestingly, treatment had no additional effect on final choice accuracy (χ^2=0.009, d.f.=1, P=0.924).

Finally, we also tested whether final choice accuracy was predicted by the initial choice at the 20 cm decision line. We found that bees that made an accurate choice at the 20 cm decision line were more likely to enter the correct reward chamber (GLMM, slope estimate±s.e.=0.65±0.25, z=2.65, P=0.008; see Table S10), demonstrating that the accuracy of early choices does predict the accuracy of final choices.

Taken together, these results suggest that acute stress influences both decision speed and outcome. Shaken bees were less likely to omit making a choice and, when they did choose, responded more quickly, especially following accurate early perception. Interestingly, these faster responses in stressed bees did not result in increased accuracy. While longer choice latencies were associated with reduced accuracy at intermediate spatial frequencies, this relationship was not further modulated by stress.

DISCUSSION

Affective states influence how visual information is processed to guide behavioural decisions. Here, we investigated whether mechanical stress that induces negative affective states alters early stages of visual processing in bees. Our results demonstrate that experience of an acute stress, potentially resembling predatory attacks, modulates visual acuity in bees. This form of stress results in reduced contrast sensitivity while improving sensitivity to finer spatial frequencies. Although these results suggest that, as in mammals, the processing of early visual features in bees can be modulated by acute stress, the direction of this modulation appears to differ.

In humans, improvements in low-level vision, and consequently lower contrast thresholds, occur following exposure to stressful threat-inducing stimuli (Phelps et al., 2006). In addition, the perception of low spatial frequencies is enhanced, while the perception of high frequencies is impaired, showing a shift in sensitivity from high to low spatial frequencies (Bocanegra and Zeelenberg, 2009). We, however, did not observe this shift in bees – both stressed and control groups maintained peak sensitivity at the trained spatial frequencies (see Fig. 2C); instead, stress flattened the response curve, extending generalisation to higher spatial frequencies, whereas controls showed a steeper decline (see Fig. 2C). While such a phenomenon is better known after absolute conditioning (Guttman and Kalish, 1956; Shepard, 1987), threat-related stimuli can also be generalised to conceptually or perceptually similar stimuli (Dunsmoor et al., 2011; Dymond et al., 2015).

Stress-enhanced processing of coarse visual features in humans has been suggested to be adaptive by leading to faster threat detection (Lojowska et al., 2019; Mermillod et al., 2010; Öhman, 2005). It might be possible that a similar function is achieved by faster processing of finer features in bees. One of the most common predators is the crab spider *Misumena vatia*, which is known to hunt while camouflaged on flowers (Dukas and Morse, 2003). Bees can use a side-to-side scanning strategy which, although time consuming and costly, improves edge detection by gradually amplifying the cryptic spider shape (Ings et al., 2012). Although our study did not test predator detection directly, the modulation of visual acuity observed here raises the possibility that acute stress alters how bees process threat-related visual features, potentially allowing them to detect finer details in their surroundings. Testing whether such changes improve detection of naturalistic stimuli, such as camouflaged predators, would be an important direction for future work.

Our threshold estimates from unmanipulated control bees show some differences to the findings of the only other visual acuity study in *B. terrestris*. The contrast threshold reported by Chakravarthi et al. (2016), 63.6%, is surprisingly high compared with the contrast threshold estimated here, which is 22%. The experimental design, including the Y-maze and stimuli, was consistent across studies. However, the luminance was substantially lower in the previous study (500 lx) compared with ours (1100 lx). As visual acuity in bees increases logarithmically with increasing light intensity (Hecht and Wolf, 1929), the contrast sensitivity threshold is also expected to change as brightness increases. The estimated spatial frequency threshold in our study, however, closely aligned with the value reported earlier. It is important to note, however, that different

accuracy criteria were used to estimate these thresholds: 65% in our study and 75% in Chakravarthi et al. (2016). Interpolating their results to a 65% accuracy criterion yields an estimated threshold of approximately 0.26 cycles deg^{-1} – very close to that observed in the present study. Moreover, bees in our study were conditioned to choose horizontally oriented stimuli, whereas Chakravarthi et al. (2016) used vertical orientations. While orientation could matter, especially given the known differences in interommatidial angle across visual planes in bees (Spaethe and Chittka, 2003), this seems unlikely, as a previous study in *Bombus impatiens* reported similar results in a detection task using both horizontal and vertical target orientations (Macuda et al., 2001). Taken together, the thresholds reported in the current study are largely aligned with earlier estimates for *B. terrestris*. Nonetheless, inconsistencies across experimental designs may help explain the observed differences.

While visual acuity thresholds capture early perception of spatial features, the final decision represents a longer-term decision-making process that is driven by increased sampling time and evidence accumulation (Usher et al., 2013). In our varying contrast trials, all bees made final choices very quickly (approximately 2.39 s at the highest and 7.27 s at the lowest contrasts; see Fig. 3A). The high accuracy and low sensitivity thresholds (see Figs 2A and 3B) observed demonstrate that the selected contrasts were well within the comfortable range of bees' vision. As discussed earlier, this is due to the high luminance levels in our study, which enabled discriminability between horizontal and vertical patterns even at the lowest contrast. Although shaking trended toward reducing choice latency, it probably could not further enhance response times that were already near ceiling values in our setup.

When it comes to varying spatial resolution, however, the effect of shaking was stronger. Shaken bees were more likely to commit to choosing (see Fig. 4A), and in some cases responded faster (see Fig. 3C), when making their final choices. Interestingly, such increased responsiveness appeared to be perception driven – significantly faster final choices were made only if the early decisions of shaken bees were correct, with this effect becoming most pronounced at the highest spatial frequencies. In spite of the expected speed–accuracy trade-off (Chittka et al., 2003; Ings and Chittka, 2008), faster choices under stress did not compromise accuracy, and we found no evidence of stress affecting performance quality. Reduced reaction times following acute stress have been reported not only in bees (Procenko et al., 2024) but also in humans (Raio et al., 2020; Wang et al., 2023), where the activation of automated responses and suppression of more deliberate decision-making processes were suggested as a driving mechanism (Raio et al., 2020). Interestingly, however, in humans, if the stressor is mild, such increased reactivity may occur without compromising accuracy, suggesting a more nuanced interaction between stress and cognition (Shields et al., 2019). Stress effects on human cognition are typically linked to hypothalamus–pituitary–adrenal axis activation. In bees, similar stress response pathways have been proposed (Even et al., 2012), which may underlie their faster yet accurate responses (Maboudi et al., 2023). One possible explanation is that shaking increased arousal via changes in biogenic amine signalling, for example involving octopamine and dopamine, both of which are implicated in arousal and attention (Even et al., 2012). Such changes could have contributed to the faster decisions observed in shaken bees, but this remains speculative and requires direct testing.

The effect of stress on visual signal processing is complex. While short-term allocation of resources to overcome acute stress tunes visual systems to better detect relevant information, the trade-off of such enhancement on more deliberate decision-making processes may be detrimental. Our study is the first to investigate these interactions in bees, which rely on vision for decision making and are continuously exposed to multiple stressors. We show that stress dynamically reshapes how bees process basic visual features and act on visual information, suggesting a broader strategy is used to adapt to uncertain environments.

Acknowledgements
The Results and Discussion in this paper are partly reproduced from the PhD thesis of O.P. (Procenko, 2024).

Competing interests
The authors declare no competing or financial interests.

Author contributions
Conceptualization: O.P., V.N.; Data curation: O.P.; Formal analysis: O.P.; Funding acquisition: V.N.; Resources: V.N.; Supervision: V.N.; Visualization: O.P.; Writing – original draft: O.P.; Writing – review & editing: V.N.

Funding
This study was funded by a Biotechnology and Biological Sciences Research Council David Phillips Fellowship (BB/S009760/1, awarded to V.N.). O.P. was supported by a PhD studentship from the Faculty of Medical Sciences, Newcastle University.

Data and resource availability
Data underlying the figures presented in the manuscript are available from figshare: https://doi.org/10.6084/m9.figshare.31982334. All other relevant data and details of resources can be found within the article and its supplementary information.

References
Bates, D., Mächler, M., Bolker, B. M. and Walker, S. C. (2015). Fitting linear mixed-effects models using lme4. *J. Stat. Softw.* **67**, 1-48. doi:10.18637/jss.v067.i01

Bateson, M., Desire, S., Gartside, S. E. and Wright, G. A. (2011). Agitated honeybees exhibit pessimistic cognitive biases. *Curr. Biol.* **21**, 1070-1073. doi:10.1016/j.cub.2011.05.017

Becker, M. W. (2009). Panic search: Fear produces efficient visual search for nonthreatening objects. *Psychol. Sci.* **20**, 435-437. doi:10.1111/j.1467-9280.2009.02303.x

Bertsch, D. J., Martin, J. P., Svenson, G. J. and Ritzmann, R. E. (2019). Predatory behavior changes with satiety or increased insulin levels in the praying mantis (*Tenodera sinensis*). *J. Exp. Biol.* **222**, jeb197673. doi:10.1242/jeb.197673

Bethell, E. J., Holmes, A., MacLarnon, A. and Semple, S. (2016). Emotion evaluation and response slowing in a non-human primate: new directions for cognitive bias measures of animal emotion? *Behav. Sci.* **6**, 2. doi:10.3390/bs6010002

Bocanegra, B. R. (2011). Emotion-induced trade-offs in spatiotemporal vision. *J. Exp. Psychol. Gen.* **140**, 272-282. doi:10.1037/a0023188

Bocanegra, B. R. and Zeelenberg, R. (2009). Emotion Improves and Impairs Early Vision. *Psychol. Sci.* **20**, 707-713. doi:10.1111/j.1467-9280.2009.02354.x

Burnham, K. P. and Anderson, D. R. (eds) (2002). *Model Selection and Multimodel Inference: Practical Information-Theoretic Approach*, 2nd edn. New York: Springer New York.

Chakravarthi, A., Baird, E., Dacke, M. and Kelber, A. (2016). Spatial vision in *Bombus terrestris*. *Front. Behav. Neurosci.* **10**, 17. doi:10.3389/fnbeh.2016.00017

Chittka, L., Dyer, A. G., Bock, F. and Dornhaus, A. (2003). Bees trade off foraging speed for accuracy. *Nature* **424**, 388. doi:10.1038/424388a

Dukas, R. and Morse, D. H. (2003). Crab spiders affect flower visitation by bees. *Oikos* **101**, 157-163. doi:10.1034/j.1600-0706.2003.12143.x

Dunsmoor, J. E., White, A. J. and LaBar, K. S. (2011). Conceptual similarity promotes generalization of higher order fear learning. *Learn. Mem.* **18**, 156-160. doi:10.1101/lm.2016411

Dymond, S., Dunsmoor, J. E., Vervliet, B., Roche, B. and Hermans, D. (2015). Fear generalization in humans: systematic review and implications for anxiety disorder research. *Behav. Ther.* **46**, 561-582. doi:10.1016/j.beth.2014.10.001

Even, N., Devaud, J. M. and Barron, A. B. (2012). General stress responses in the honey bee. *Insects* **3**, 1271-1298. doi:10.3390/insects3041271

Fox, J., Weisberg, S. and Price, B. (2019). *An R Companion to Applied Regression*, 3rd edn. Thousand Oaks, CA: Sage.

Friard, O. and Gamba, M. (2016). BORIS: a free, versatile open-source event-logging software for video/audio coding and live observations. *Methods Ecol. Evol.* **7**, 1325-1330. doi:10.1111/2041-210X.12584

Guttman, N. and Kalish, H. (1956). Discriminability and stimulus generalization. *J. Exp. Psychol.* **51**, 79-88. doi:10.1037/h0046219

Hecht, B. Y. S. and Wolf, E. (1929). The visual acuity of the honey bee. *J. Gen. Physiol.* **12**, 727-760. doi:10.1085/jgp.12.6.727
Hindmarsh Sten, T., Li, R., Otopalik, A. and Ruta, V. (2021). Sexual arousal gates visual processing during *Drosophila* courtship. *Nature* **595**, 549-553. doi:10.1038/s41586-021-03714-w
Ings, T. C. and Chittka, L. (2008). Speed-accuracy tradeoffs and false alarms in bee responses to cryptic predators. *Curr. Biol.* **18**, 1520-1524. doi:10.1016/j.cub.2008.07.074
Ings, T. C., Wang, M. Y. and Chittka, L. (2012). Colour-independent shape recognition of cryptic predators by bumblebees. *Behav. Ecol. Sociobiol.* **66**, 487-496. doi:10.1007/s00265-011-1295-y
Johnson, J. B. and Omland, K. S. (2004). Model selection in ecology and evolution. *Trends Ecol. Evol.* **19**, 101-108. doi:10.1016/j.tree.2003.10.013
Kiani, R., Corthell, L. and Shadlen, M. N. (2014). Choice certainty is informed by both evidence and decision time. *Neuron* **84**, 1329-1342. doi:10.1016/j.neuron.2014.12.015
Kim, A. J., Lee, D. S. and Anderson, B. A. (2021). The influence of threat on the efficiency of goal-directed attentional control. *Psychol. Res.* **85**, 980-986. doi:10.1007/s00426-020-01321-4
Lee, T. H., Baek, J., Lu, Z. L. and Mather, M. (2014). How arousal modulates the visual contrast sensitivity function. *Emotion* **14**, 978-984. doi:10.1037/a0037047
Linares, D. and López-Moliner, J. (2016). quickpsy: An R package to fit psychometric functions for multiple groups. *R J.* **8**, 122-131. doi:10.32614/RJ-2016-008
Lojowska, M., Mulckhuyse, M., Hermans, E. J. and Roelofs, K. (2019). Unconscious processing of coarse visual information during anticipatory threat. *Conscious. Cogn.* **70**, 50-56. doi:10.1016/j.concog.2019.01.018
Longden, K. D., Muzzu, T., Cook, D. J., Schultz, S. R. and Krapp, H. G. (2014). Nutritional state modulates the neural processing of visual motion. *Curr. Biol.* **24**, 890-895. doi:10.1016/j.cub.2014.03.005
Maboudi, H., Marshall, J. A. R., Dearden, N. and Barron, A. B. (2023). How honey bees make fast and accurate decisions. *eLife* **12**, e86176. doi:10.7554/eLife.86176
Macuda, T., Gegear, R. J., Laverty, T. M. and Timney, B. (2001). Behavioural assessment of visual acuity in bumblebees (*Bombus impatiens*). *J. Exp. Biol.* **204**, 559-564. doi:10.1242/jeb.204.3.559
Magnusson, A., Skaug, H. J., Nielsen, A., Berg, C., Kristensen, K., Maechler, M., Van Bentham, K., Bolker, B. and Brooks, M. (2017). glmmTMB balances speed and flexibility among packages for zero-inflated generalized linear mixed modeling. *R J.* **9**, 378-400. doi:10.32614/RJ-2017-066
Maimon, G., Straw, A. D. and Dickinson, M. H. (2010). Active flight increases the gain of visual motion processing in *Drosophila*. *Nat. Neurosci.* **13**, 393-399. doi:10.1038/nn.2492
Mermillod, M., Droit-volet, S., Devaux, D., Schaefer, A. and Vermeulen, N. (2010). Are coarse scales sufficient for fast detection of visual threat? *Psychol. Sci.* **21**, 1429-1437. doi:10.1177/0956797610381503
Öhman, A. (2005). The role of the amygdala in human fear: automatic detection of threat. *Psychoneuroendocrinology* **30**, 953-958. doi:10.1016/j.psyneuen.2005.03.019
Phelps, E. A., Ling, S. and Carrasco, M. (2006). Emotion facilitates perception and potentiates the perceptual benefits of attention. *Psychol. Sci.* **17**, 292-299. doi:10.1111/j.1467-9280.2006.01701.x
Procenko, O. (2024). Affective state and visual decision-making in bumblebees. *PhD thesis*, Newcastle University. http://theses.ncl.ac.uk/jspui/handle/10443/6474
Procenko, O., Read, J. C. A. and Nityananda, V. (2024). Physically stressed bees expect less reward in an active choice judgement bias test. *Proc. R. Soc. B Biol. Sci.* **291**, 20240512. doi:10.1098/rspb.2024.0512
Raio, C. M., Konova, A. B. and Otto, A. R. (2020). Trait impulsivity and acute stress interact to influence choice and decision speed during multi-stage decision-making. *Sci. Rep.* **10**, 7754. doi:10.1038/s41598-020-64540-0
Rosner, R., Egelhaaf, M. and Warzecha, A. K. (2010). Behavioural state affects motion-sensitive neurones in the fly visual system. *J. Exp. Biol.* **213**, 331-338. doi:10.1242/jeb.035386
Rued, H. A., Hilmert, C. J., Strahm, A. M. and Thomas, L. E. (2019). The influence of stress on attentional bias to threat: an angry face and a noisy crowd. *Psychon. Bull. Rev.* **26**, 943-950. doi:10.3758/s13423-018-1538-2
Schlüns, H., Welling, H., Federici, J. R. and Lewejohann, L. (2017). The glass is not yet half empty: agitation but not Varroa treatment causes cognitive bias in honey bees. *Anim. Cogn.* **20**, 233-241. doi:10.1007/s10071-016-1042-x
Schwarz, N. and Clore, G. L. (1983). Mood, misattribution, and judgments of well-being: Informative and directive functions of affective states. *J. Pers. Soc. Psychol.* **45**, 513-523. doi:10.1037/0022-3514.45.3.513
Shepard, R. N. (1987). Toward a universal law of generalization for psychological science. *Science* **237**, 1317-1323. doi:10.1126/science.3629243
Shields, G. S., Rivers, A. M., Ramey, M. M., Trainor, B. C. and Yonelinas, A. P. (2019). Mild acute stress improves response speed without impairing accuracy or interference control in two selective attention tasks: Implications for theories of stress and cognition. *Psychoneuroendocrinology* **108**, 78-86. doi:10.1016/j.psyneuen.2019.06.001
Spaethe, J. and Chittka, L. (2003). Interindividual variation of eye optics and single object resolution in bumblebees. *J. Exp. Biol.* **206**, 3447-3453. doi:10.1242/jeb.00570
Usher, M., Tsetsos, K., Yu, E. C. and Lagnado, D. A. (2013). Dynamics of decision-making: from evidence accumulation to preference and belief. *Front. Psychol.* **4**, 758. doi:10.3389/fpsyg.2013.00758
Wang, J., Yu, L., Ding, F. and Qi, C. (2023). Effect of acute psychological stress on speed perception: an event-related potential study. *Brain Sci.* **13**, 423. doi:10.3390/brainsci13030423
Zadra, J. R. and Clore, G. L. (2011). Emotion and perception: The role of affective information. *Wiley Interdiscip. Rev. Cogn. Sci.* **2**, 676-685. doi:10.1002/wcs.147

Table S1. Summary and comparison of generalized linear mixed-effects models assessing bee accuracy in crossing a 20 cm decision line on varying contrast trials.

Selection of best-fit model

Model	Dependent variable	Fixed factors	Random factor	*df*	*AIC*	*ΔAIC*
model 1	**Accuracy**	**Treatment+Contrast+Eye length**	ID	**5**	**149.34**	**0**
model 2	Accuracy	Treatment+Contrast*Eye length	ID	6	150.255	0.915
model 3	Accuracy	Treatment*Eye length+contrast	ID	6	150.883	1.542
model 4	Accuracy	Treatment*Contrast+Eye length	ID	6	150.99	1.65
model 5	Accuracy	Treatment*Contrast*Eye length	ID	9	154.391	5.051

Follow-up likelihood ratio test comparing models

Model	Parameters	Deviance	X^2	*df*	*P*
model 1	5	139.34			
model 2	6	138.25	1.086	1	0.298
model 3	6	138.88	0	0	1
model 4	6	138.99	0	0	1

Summary of model coefficients with standard errors and significance tests

Term	Estimate	SE	*z*	*P*
(Intercept)	2.083	6.165	0.338	0.735
Treatment Shaking	-0.41	0.505	-0.811	0.417
Contrast	**0.03**	**0.011**	**2.761**	**0.006**
Eye length	-0.498	2.309	-0.216	0.829

The tables present the best-fitting generalized linear mixed-effects models, including fixed and random effects, degrees of freedom (df), and Akaike's Information Criterion (AIC). The model with the lowest AIC was selected as best. However, if competing models had a ΔAIC < 2, they were considered statistically indistinguishable (Burnham & Anderson, 2004), and the simpler model was preferred. In such cases, a follow-up likelihood ratio test was used to compare model fit. The final selected model appears in bold. P < 0.05 indicates statistical significance.

Journal of Experimental Biology • Supplementary information

Table S2. Summary and comparison of generalized linear mixed-effects models assessing bee latency to cross 20 cm decision line on varying contrast trials.

Selection of best-fit model

Model	Dependent variable	Fixed factors	Random factor	*df*	*AIC*	*ΔAIC*
model 1	log(latency)	Treatment+Contrast	ID	8	348.944	0
model 2	**log(latency)**	**Treatment*Contrast**	**ID**	**12**	**350.702**	**1.758**

Follow-up likelihood ratio test comparing models

Model	Parameters	Deviance	X^2	*df*	*P*
model 1	8	315.2			
model 2	**12**	**302.37**	**12.83**	**4**	**0.012**

Summary of model coefficients with standard errors and significance tests

Term	Estimate	SE	*t*	*df*	*P*
(Intercept)	-0.958	0.128	-7.483	133.946	0.000
Treatment Shaking	0.182	0.181	1.006	133.946	0.316
Contrast 22%	0.14	0.149	0.935	150.174	0.351
Contrast 39%	0.133	0.149	0.892	150.174	0.374
Contrast 54%	0.132	0.149	0.886	150.174	0.377
Contrast 68%	0.065	0.151	0.427	150.791	0.67
Treatment Shaking:Contrast 22%	-0.115	0.211	-0.545	150.174	0.587
Treatment Shaking:Contrast 39%	-0.142	0.211	-0.674	150.174	0.501
Treatment Shaking:Contrast 54%	**-0.675**	**0.213**	**-3.176**	**150.487**	**0.002**
Treatment Shaking:Contrast 68%	-0.086	0.213	-0.403	150.487	0.688

Type II Wald chi-square tests for fixed effects.

Effect	X^2	*df*	*P*
Treatment	0.025	1	0.874
factor(contrast)	8.837	4	0.065
Treatment:factor(contrast)	12.685	4	0.013

Bonferroni-corrected post hoc tests for Treatment × Contrast interaction

Frequency (Level)	*Estimate*	*SE*	*df*	*t*	*P*
87	-0.182	0.181	133.736	-1.006	0.316
68	-0.096	0.183	136.13	-0.527	0.599
54	**0.493**	**0.183**	**136.13**	**2.697**	**0.008**
39	-0.04	0.181	133.736	-0.22	0.826
22	-0.067	0.181	133.736	-0.371	0.711

The tables present the best-fitting generalized linear mixed-effects models, including fixed and random effects, degrees of freedom (df), and Akaike's Information Criterion (AIC). The model with the lowest AIC was selected as best. However, if competing models had a ΔAIC < 2, they were considered statistically indistinguishable (Burnham & Anderson, 2004), and the simpler model was preferred. In such cases, a follow-up likelihood ratio test was used to compare model fit. The final selected model appears in bold. P < 0.05 indicates statistical significance.

Journal of Experimental Biology • Supplementary information

Table S3. Summary and comparison of generalized linear mixed-effects models assessing accuracy in correctly crossing the 20 cm decision line on varying spatial frequency trials.

Selection of best-fit model

Model	Dependent variable	Fixed factors	Random factor	*df*	*AIC*	*ΔAIC*
model 1	**Accuracy**	**Treatment+frequency+Eye length**	**ID**	**9**	**396.995**	**0**
model 2	Accuracy	Treatment*Eye length+Frequency	ID	10	397.498	0.502
model 3	Accuracy	Treatment*Frequency+Eye length	ID	14	403.668	6.673
model 4	Accuracy	Treatment+Frequency*Eye length	ID	14	404.174	7.178
model 5	Accuracy	Treatment*Frequency*Eye length	ID	25	418.684	21.688

Follow-up likelihood ratio test comparing models

Model	Parameters	Deviance	X^2	*df*	*P*
model 1	**9**	**379**			
model 2	10	377.5	1.498	1	0.221

Summary of model coefficients with standard errors and significance tests

Term	Estimate	*SE*	*z*	*P*
(Intercept)	10.255	4.267	2.403	0.016
Treatment Shaking	0.298	0.328	0.906	0.365
Frequency 035 deg^{-1}	-1.48	0.717	-2.064	0.039
Frequency 0.14 deg^{-1}	-0.723	0.693	-1.043	0.297
Frequency 0.28 deg^{-1}	-2.2	0.658	-3.342	0.001
Frequency 0.437 deg^{-1}	-2.21	0.66	-3.347	0.001
Frequency 0.699 deg^{-1}	-2.682	0.7	-3.832	0
Eye length	-2.89	1.579	-1.83	0.067

Type II Wald chi-square tests for fixed effects

Effect	X^2	*df*	*P*
Treatment	0.821	1	0.365
Frequency	**30.543**	**5**	**0.000**
Eye length	3.349	1	0.067

The tables present the best-fitting generalized linear mixed-effects models, including fixed and random effects, degrees of freedom (df), and Akaike's Information Criterion (AIC). The model with the lowest AIC was selected as best. However, if competing models had a ΔAIC < 2, they were considered statistically indistinguishable (Burnham & Anderson, 2004), and the simpler model was preferred. In such cases, a follow-up likelihood ratio test was used to compare model fit. The final selected model appears in bold. P < 0.05 indicates statistical significance.

Journal of Experimental Biology • Supplementary information

Table S4. Summary and comparison of generalized linear mixed-effects models assessing bee latency to cross 20 cm decision line on varying spatial frequency trials.

Selection of best-fit model

Model	Dependent variable	Fixed factors	Random factor	*df*	*AIC*	*ΔAIC*
model 1	**log(latency)**	**Treatment+Frequency**	**ID**	**9**	**584.446**	**0**
model 2	log(latency)	Treatment*Frequency	ID	14	601.475	17.029

Summary of model coefficients with standard errors and significance tests

Term	Estimate	*SE*	*t*	*df*	*P*
(Intercept)	-0.885	0.11	-8.022	106.317	0
Treatment: Shaking	0.037	0.119	0.309	38.225	0.759
Frequency 0.035 deg-1	-0.025	0.107	-0.234	308.231	0.815
Frequency 0.14 deg-1	-0.048	0.093	-0.514	308.354	0.608
Frequency 0.28 deg-1	0.051	0.093	0.549	308.292	0.583
Frequency 0.437 deg-1	**0.183**	**0.094**	**1.952**	**308.467**	**0.052**
Frequency 0.699 deg-1	**0.229**	**0.107**	**2.138**	**308.231**	**0.033**

The tables present the best-fitting generalized linear mixed-effects models, including fixed and random effects, degrees of freedom (df), and Akaike's Information Criterion (AIC). The model with the lowest AIC was selected as best. However, if competing models had a ΔAIC < 2, they were considered statistically indistinguishable (Burnham & Anderson, 2004), and the simpler model was preferred. In such cases, a follow-up likelihood ratio test was used to compare model fit. The final selected model appears in bold. P < 0.05 indicates statistical significance.

Journal of Experimental Biology • Supplementary information

Table S5. Summary and comparison of generalized linear mixed-effects models assessing bees' final choice outcomes (correct, incorrect, or omission when choosing which of two rewarding chambers to enter) across varying contrast trials.

Selection of best-fit model

Model	Dependent variable	Fixed factors	Random factor	*df*	*AIC*	*ΔAIC*
model 1	**YesNo**	**Type + Treatment**	**ID**	**5**	**391.179**	**0**
model 2	YesNo	Type * Treatment	ID	7	392.407	1.228

Follow-up likelihood ratio test comparing models

Model	Parameters	Deviance	X^2	*df*	*P*
model 1	5	381.179			
model 2	7	378.407	2.772	2	0.25

Summary of model coefficients with standard errors and significance tests

Term	Estimate	*SE*	*z*	*P*
(Intercept)	1.589	0.23	6.903	0.000
Treatment Shaking	-0.021	0.265	-0.078	0.938
Incorrect choice	**-3.255**	**0.269**	**-12.084**	**0.000**
Choice omission	**-6.149**	**0.736**	**-8.363**	**0.000**

Type II Wald chi-square tests for fixed effects

Effect	X^2	*df*	*P*
Type	**185.731**	**2**	**0.000**
Treatment	0.006	1	0.938

The tables present the best-fitting generalized linear mixed-effects models, including fixed and random effects, degrees of freedom (df), and Akaike's Information Criterion (AIC). The model with the lowest AIC was selected as best. However, if competing models had a ΔAIC < 2, they were considered statistically indistinguishable (Burnham & Anderson, 2004), and the simpler model was preferred. In such cases, a follow-up likelihood ratio test was used to compare model fit. The final selected model appears in bold. P < 0.05 indicates statistical significance.

Journal of Experimental Biology • Supplementary information

Table S6. Summary and comparison of generalized linear mixed-effects models assessing bees' final choice latency during varying contrast trials.

Selection of best-fit model

Model	Dependent variable	Fixed factors	Random factor	*df*	*AIC*	*ΔAIC*
model 1	**Latency $^{-1}$**	**Treatment+Contrast+Accuracy**	**ID**	**6**	**-68.626**	**0**
model 2	Latency $^{-1}$	Treatment*Accuracy+Contrast	ID	7	-63.881	4.746
model 3	Latency $^{-1}$	Treatment+Contrast*Accuracy	ID	7	-55.904	12.722
model 4	Latency $^{-1}$	Treatment*Contrast+Accuracy	ID	7	-54.909	13.717
model 5	Latency $^{-1}$	Treatment*Contrast*Accuracy	ID	10	-26.131	42.496

Summary of model coefficients with standard errors and significance tests

Term	Estimate	*SE*	*t*	*df*	*P*
(Intercept)	0.077	0.05	1.548	169.141	0.124
Treatment: Shaking	0.069	0.038	1.807	38.235	0.079
Contrast	**0.003**	**0.001**	**4.83**	**154.74**	**0.000**
Correct choice	0.036	0.041	0.886	180.986	0.377

Type II Wald chi-square tests for fixed effects

Effect	X^2	*df*	*P*
Treatment	3.264	1	0.071
Contrast	**23.331**	**1**	**0.000**
Accuracy	0.786	1	0.375

The tables present the best-fitting generalized linear mixed-effects models, including fixed and random effects, degrees of freedom (df), and Akaike's Information Criterion (AIC). The model with the lowest AIC was selected as best; however, if competing models had a ΔAIC < 2, they were considered statistically indistinguishable (Burnham & Anderson, 2004), and the simpler model was preferred. In such cases, a follow-up likelihood ratio test was used to compare model fit. The final selected model appears in bold. P < 0.05 indicates statistical significance.

Table S7. Summary and comparison of generalized linear mixed-effects models assessing bees' final choice outcomes (correct, incorrect, or omission when choosing which of two rewarding chambers to enter) across varying spatial frequency trials.

Selection of best-fit model

Model	Dependent variable	Fixed factors	Random factor	*df*	*AIC*	*ΔAIC*
model 1	**YesNo**	**Treatment*Type**	**ID**	**7**	**846.492**	**0.000**
model 2	YesNo	Treatment+Type	ID	5	853.253	6.761

Type II Wald chi-square tests for fixed effects

Effect	X^2	*df*	*P*
Treatment	0.024	1	0.878
Type	**328.28**	**2**	**0.000**
Treatment x Type	**9.775**	**2**	**0.008**

Bonferroni-corrected paired post hoc comparison for Treatment × Type interaction

Level	Estimate	*SE*	*df*	*z*	*P*
Correct	**-0.518**	**0.261**	**Inf**	**-1.986**	**0.047**
Incorrect	0.196	0.29	Inf	0.676	0.499
Omission	**1.218**	**0.524**	**Inf**	**2.323**	**0.02**

The tables present the best-fitting generalized linear mixed-effects models, including fixed and random effects, degrees of freedom (df), and Akaike's Information Criterion (AIC). The model with the lowest AIC was selected as best. However, if competing models had a ΔAIC < 2, they were considered statistically indistinguishable (Burnham & Anderson, 2004), and the simpler model was preferred. In such cases, a follow-up likelihood ratio test was used to compare model fit. The final selected model appears in bold. $P < 0.05$ indicates statistical significance.

Journal of Experimental Biology • Supplementary information

Table S8. Summary and comparison of generalized linear mixed-effects models assessing bees' final choice latency during varying spatial frequency trials.

Selection of best-fit model

Model	Dependent variable	Fixed factors	Random factor	*df*	*AIC*	*ΔAIC*
model 1	**log(latency)**	**Treatment*Accuracy+Frequency**	**ID**	**11**	**881.541**	**0**
model 2	log(latency)	Treatment+Frequency+Accuracy	ID	10	885.405	3.863
model 3	log(latency)	Treatment*Frequency*Accuracy	ID	26	885.655	4.114
model 4	log(latency)	Treatment+Frequency*Accuracy	ID	15	892.062	10.521
model 5	log(latency)	Treatment*Frequency+Accuracy	ID	15	892.963	11.421

Summary of model coefficients with standard errors and significance tests

Term	Estimate	*SE*	*t*	*df*	*P*
(Intercept)	1.127	0.205	5.496	281.126	0.000
Treatment Shaking	-0.009	0.197	-0.045	143.375	0.964
Correct choice	0.171	0.161	1.063	315.192	0.289
Frequency 0.035 deg-1	0.782	0.197	3.964	278.983	0.000
Frequency 0.14 deg-1	1.154	0.17	6.798	278.082	0.000
Frequency 0.28 deg-1	1.77	0.174	10.165	281.182	0.000
Frequency 0.437 deg-1	1.915	0.179	10.719	283.577	0.000
Frequency 0.699 deg-1	2.163	0.212	10.218	284.784	0.000
Treatment Shaking:Correct choice	-0.581	0.217	-2.672	315.028	0.008

Type II Wald chi-square tests for fixed effects

Effect	X^2	*df*	*P*
Treatment	11.029	1	0.001
Accuracy	1.333	1	0.248
Frequency	173.049	5	0
Treatment:Accuracy	7.138	1	0.008

Bonferroni-corrected paired post hoc comparison for Treatment × Type interaction

Level	Estimate	*SE*	*df*	*z*	*P*
Incorrect crossing	0.009	0.198	146.359	0.044	0.965
Correct crossing	0.59	0.141	57.646	4.176	0

The tables present the best-fitting generalized linear mixed-effects models, including fixed and random effects, degrees of freedom (df), and Akaike's Information Criterion (AIC). The model with the lowest AIC was selected as best. However, if competing models had a ΔAIC < 2, they were considered statistically indistinguishable (Burnham & Anderson, 2004), and the simpler model was preferred. In such cases, a follow-up likelihood ratio test was used to compare model fit. The final selected model appears in bold. $P < 0.05$ indicates statistical significance.

Table S9. Summary and comparison of generalized linear mixed-effects models assessing bee final choice accuracy on varying spatial frequency trials.

Selection of best-fit model

Model	Dependent variable	Fixed factors	Random factor	*df*	*AIC*	*ΔAIC*
model 1	**Accuracy**	**Latency*Frequency+Treatment**	**ID**	**14**	**286.736**	**0**
model 2	Accuracy	Latency+Frequency+Treatment	ID	9	290.836	4.1
model 3	Accuracy	Latency*Treatment+Frequency	ID	10	292.505	5.77
model 4	Accuracy	Frequency*Treatment+Latency	ID	14	292.688	5.952
model 5	Accuracy	Latency*Frequency+Latency *Treatment+Frequency *Treatment	ID	20	293.215	6.48

Type II Wald chi-square tests for fixed effects.

Effect	X^2	*df*	*P*
Latency	**5.766**	**1**	**0.016**
Frequency	5.584	5	0.349
Treatment	0.009	1	0.924
Latency x Frequency	**11.143**	**5**	**0.049**

Post hoc estimates of slopes for the Latency × Frequency interaction, showing the effect of latency on probability of entering incorrect reward chamber at each spatial frequency level.

Frequency	*Estimate*	*SE*	*z*	*P*
0.035 cycles deg^{-1}	-0.026	0.199	-0.13	0.897
0.28 cycles deg^{-1}	**-0.037**	**0.017**	**-2.142**	**0.032**
0.14 cycles deg^{-1}	**-0.081**	**0.029**	**-2.762**	**0.006**
0.437 cycles deg^{-1}	-0.01	0.009	-1.007	0.314
0.07 cycles deg^{-1}	-0.02	0.013	-1.601	0.109
0.699 cycles deg^{-1}	0.037	0.025	1.484	0.138

The tables present the best-fitting generalized linear mixed-effects models, including fixed and random effects, degrees of freedom (df), and Akaike's Information Criterion (AIC). The model with the lowest AIC was selected as best. However, if competing models had a ΔAIC < 2, they were considered statistically indistinguishable (Burnham & Anderson, 2004), and the simpler model was preferred. In such cases, a follow-up likelihood ratio test was used to compare model fit. The final selected model appears in bold. P < 0.05 indicates statistical significance.

Journal of Experimental Biology • Supplementary information

Table S10. Summary and comparison of generalized linear mixed-effects models assessing the effect of bees' accuracy in crossing the 20 cm decision line on final choice accuracy.

Selection of best-fit model

Model	Dependent variable	Fixed factors	Random factor	*df*	*AIC*	*ΔAIC*
model 1	**Accuracy to enter**	Accuracy to cross 20 cm	**ID**	**3**	**588.46**	**0**
model 2	Accuracy to enter	Accuracy to cross 20 cm+Treatment+Cue	ID	17	599.37	10.907
model 3	Accuracy to enter	Accuracy to cross 20 cm*Treatment+Cue	ID	18	601.25	12.785
model 4	Accuracy to enter	Accuracy to cross 20 cm*Cue	ID	29	605.34	16.068
model 5	Accuracy to enter	Accuracy to cross 20 cm+Treatment*Cue	ID	30	605.53	17.068
model 6	Accuracy to enter	Accuracy to cross 20 cm*Cue+Treatment	ID	30	606.61	18.148

Summary of model coefficients with standard errors and significance tests

Term	Estimate	*SE*	*z*	*P*
(Intercept)	1.147	0.237	4.843	0.000
Accuracy to cross 20 cm	**0.650**	0.246	**2.649**	**0.008**

The tables present the best-fitting generalized linear mixed-effects models, including fixed and random effects, degrees of freedom (df), and Akaike's Information Criterion (AIC). The model with the lowest AIC was selected as best. However, if competing models had a ΔAIC < 2, they were considered statistically indistinguishable (Burnham & Anderson, 2004), and the simpler model was preferred. In such cases, a follow-up likelihood ratio test was used to compare model fit. The final selected model appears in bold. P < 0.05 indicates statistical significance.

Journal of Experimental Biology • Supplementary information